

NANOCOMPOSITE MATERIALS: FUTURE AND CHALLENGE FOR THE PRODUCTION OF THERMOELECTRIC DEVICES

D.G. Ebling¹, A. Jacquot¹, H. Böttner¹, J. Schmidt², P. Spies³

¹Fraunhofer-Institut für Physikalische Messtechnik IPM, Department of Thermoelectric Systems, Freiburg, Germany

²Fraunhofer-Institut für Fertigungstechnik und Angewandte Materialforschung IFAM, Institutsteil Dresden, Germany

³Fraunhofer-Institut für Integrierte Schaltungen IIS, Erlangen, Germany

Abstract: In this paper the evolution of thermoelectric material parameters of V-VI and V-VI/IV_VI compounds like thermal and electrical conductivity, Seebeck coefficient and the dimensionless figure of merit (ZT) is discussed in dependence on the fabrication and doping of the base material as well as on the treatment during and after preparation using melt spinning and sparc plasma sintering (SPS). This material is used as the basis for the fabrication of thermoelectric modules to be integrated into power supplies for the operation of wireless sensors. They employ particularly tailored dc-dc-converter topologies which are configured to cope with extremely low input voltage sources.

Key Words: Nanocomposite, sparc plasma sintering (SPS), melt spin, bismuth telluride, lead telluride, wireless sensors

1. INTRODUCTION

The preparation of thermoelectric compounds of doped bismuth telluride and its alloys has recently gained increasing interest due to their structural features showing increased values for the thermoelectric figure of merit (ZT) [1, 2].

One promising approach to improve the thermoelectric properties is to manufacture nanocomposite materials exhibiting lower thermal conductivities and higher ZT values. The use of nanostructured materials has led to recent breakthroughs in the thermoelectric field [1–3].

Beside the possibility to grow nanoscaled materials by epitaxial methods, it is attractive to produce much cheaper bulk materials with a nanoscaled structure exhibiting similar profits for thermoelectric applications. Mainly two basic methods are described. One is based on mechanical alloying and subsequent sintering of those mixtures [4], the other one is based on rapid cooling of homogeneous multi component melts exhibiting large miscibility gaps in solid state in the corresponding phase diagram, which will form nanoscaled precipitations in a bulk sample under those conditions. [5-9]

Melt spinning, developed for rapid cooling of liquids like metal melts, is used to develop materials that require extremely high cooling rates in order to form, such as metallic glasses or

nanocomposites. The cooling rates achievable by melt-spinning are in the order of 10^1 - 10^7 Kelvin/s.

The multi component system of PbTe/Bi₂Te₃/Sb₂Te₃/Bi₂Se₃ is of special interest being composed of good thermoelectric materials on the one hand but with a restricted miscibility in the phase diagram e.g. PbTe/ Bi₂Te₃ [10, 11, 15]. The miscibility in phase diagrams may even differ severely for different authors, also indicating a high uncertainty of the crystalline fine structure on the nanoscale. [10-15]. Thus, it is worth to examine those nanocomposites of „V₂VI₃“ with PbTe bulk quenched material in detail to compare the results to the corresponding melt spin material.

These materials are not ready for the production of thermoelectric device due to their poor mechanical properties. The possibility to sinter materials almost without grain growth makes the sparc plasma sintering (SPS) -process (figure 1) a relevant technique for the compaction of nanostructured powders. During the later phase of sintering Joule's heat is generated due to the current flow especially at places of high electrical resistance and temporarily overheats the sample while the overall sintering temperature is relatively low [8, 9].

Spark Plasma Sintering



Sample-Ø: 40 ... 300 mm
Sample height: 10 ... 80 mm
Pressure: 250 / 40 t
Current: 60 000 A
Voltage: 10 V
Atmosphere: N₂, Ar
Vacuum: 5·10⁻² mbar

Fig. 1: Front view of the equipment for the spark plasma sintering process with some equipment specifications.

In contrast to other sintering techniques a special preparation of the sample, i.e. by cold pressing, is not necessary, because the powder is filled directly in the mould. That makes the method very valuable for production processes with high material throughput. For material produced under these conditions a ZT value better than 1 could already be obtained [16].

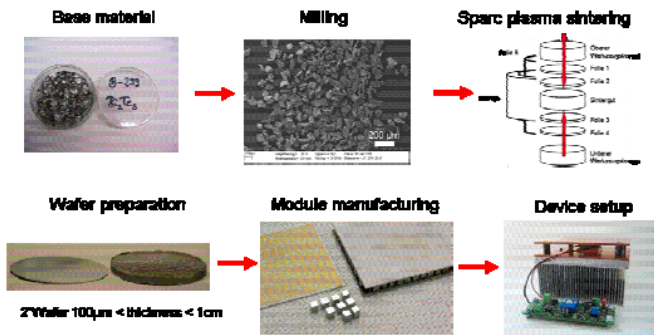


Figure 2: Complete manufacturing chain for thermoelectric driven self sustaining sensors.

We will discuss the fabrication of thermoelectric devices, see also fig.2, based on SPS material.

Due to the properties, the material is applicable to various kinds of thermoelectric devices. A very important application field focused by Fraunhofer IPM is the energy supply to remote sensing units combined with wireless data transfer. We used this material as the basis for the fabrication of modules to be integrated into thermoelectrically power supplies which employ particularly tailored dc-dc-converter topologies and which are configured to cope with extremely low input voltage sources. The complete manufacturing chain from the material to the final device is given in figure 2.

Small sized thermo generators as well as small temperature differences can be used to supply electrical circuits. In addition, first results on the performance of the thermoelectric generators in dependence of the material quality will be discussed.

2. SPS-WAFER PREPARATION AND STRUCTURAL PROPERTIES

The wafers were prepared by milling the commercial source materials which were ingots or melt spin material of p-type (Bi_{0.2}Sb_{0.8})₂Te₃ and of n-type Bi₂(Se,Te)₃. By optimizing the spark plasma sintering conditions we were able to produce SPS-wafers with reproducible properties. Standard wafers have a diameter of 45 mm and a thickness of about 3 mm, which can be set to 1mm at its lowest and to more than 15 mm if needed. The thickness of the wafer can be adjusted to a maximum variation of less than 2%, which leads to the possibility to use them directly for production without an additional polishing step.

The lateral homogeneity of the wafers was analyzed by measuring the thermoelectrical properties. One wafer was cut into pieces to determine the Seebeck coefficient in figure 3.

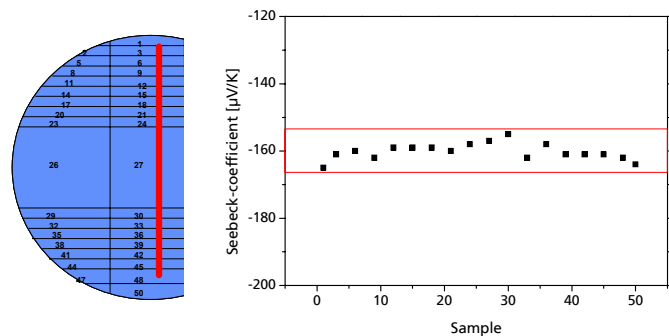


Fig. 3: Homogeneity of a n-type SPS-wafer. On the left hand side the positions of the measured samples cut from the SPS-wafer are indicated by a red line.

As can be seen from figure 3, the deviation is less than 5% which corresponds to the uncertainty of the measurement. Thus, the homogeneity has to be considered as quite good. To study the influence of the SPS-process, the properties of the SPS-wafer were analyzed in the direction of the pressure force and perpendicular, which means perpendicular to the wafer surface or parallel,

respectively.

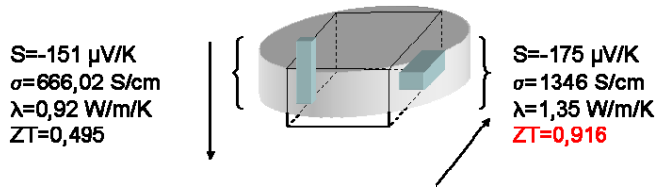


Fig. 4: Scheme of the oriented sample preparation from a SPS-wafer, incl. data indicating a textured morphology.

Samples were cut from a 15mm thick wafer according to the drawing, figure 4. While the Seebeck coefficient remained more or less the same for both directions, anisotropic behavior was found for the electrical and thermal conductivity. The electrical conductivity is nearly doubled up to a value of $1346 (\Omega \cdot \text{cm})^{-1}$. Comparing samples parallel to the pressure direction with perpendicular ones, the thermal conductivity increased only by a factor of about 1.5. This results in nearly doubling the figure of merit to a value of 0.92 for samples perpendicular to the pressure force direction. This is in good agreement with single crystal measurements [1], showing isotropic behavior of the Seebeck coefficient for all compounds in the system $(\text{Bi}, \text{Sb})_2(\text{Se}, \text{Te})_3$ and an increase of thermal conductivity by a factor of 1.8 to 2.5 and of electrical conductivity by a factor of 2.5 to 6.7 due to the anisotropic physical properties.[17]

3. ALLOYING OF $(\text{Bi}, \text{Sb})_2\text{Te}_3$ WITH PbTe

To improve the thermoelectric properties of the material Bi_2Te_3 compounds were alloyed with PbTe as a promising possibility to form nanocomposites. The concentration of PbTe was varied between 0.05 at% and 0.5 at%, which is still in a range where some authors predict miscibility of these compounds in solid state [10].

The samples were prepared by melting the starting materials with appropriate initial weight in a quartz ampoule together; the ampoules were quenched into cold water. The light microscopic and SEM inspection of the samples showed no evidence of any precipitation or inclusions down to the sub micron range.

Also annealing of the samples did not produce any precipitation in that range. TEM inspection of

the material is still in preparation and will be published elsewhere.

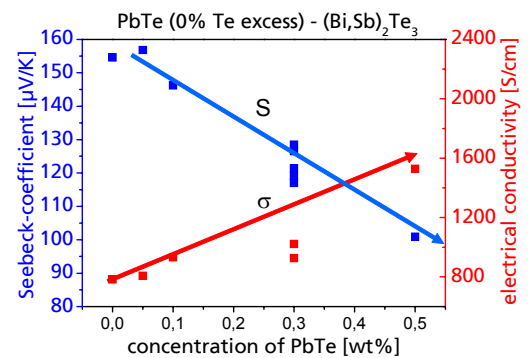


Fig. 5: Influence of the amount of PbTe alloying on the thermoelectric properties of in water quenched p-type $(\text{Bi}_{0.2}\text{Sb}_{0.8})_2\text{Te}_3$. Lines are guides to the eye.

The thermoelectric properties are shown in figure 5. All samples are p-type. By increasing the amount of PbTe the Seebeck coefficient is reduced from about 160 to 100 $\mu\text{V}/\text{K}$ while the electrical conductivity is increased from about 800 to 1600 S/cm , which might be explained by a doping effect due to the PbTe.

The thermoelectric properties were analysed parallel to the surface at room temperature (RT) for p-type samples with PbTe up to 0.5%. The thermal conductivity of these samples shows a minimum for a concentration of 0.1% PbTe for

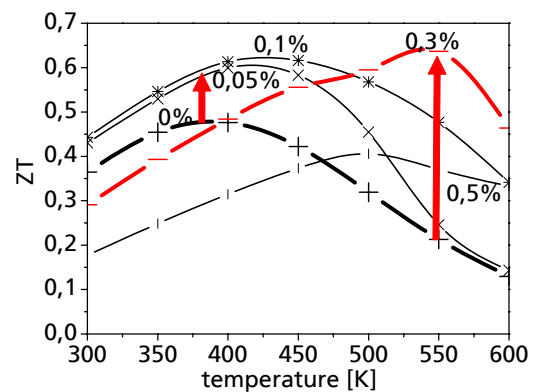


Fig. 6: Figure of merit ZT for p-type $(\text{Bi}_{0.2}\text{Sb}_{0.8})_2\text{Te}_3$ with different concentrations of PbTe depending on measuring temperature. A clear improvement of ZT is observed for low concentrations of PbTe close to RT and for higher concentrations at elevated temperature up to 600 K, indicated by red arrows.

temperatures from RT to 600K.

This leads to an improvement of the figure of merit ZT at RT of about 20% ($ZT=0.45$) compared to the samples without PbTe (fig. 6). While that improvement at RT is most likely due to the improved electrical and reduced thermal conductivity, the increase by a factor of 3 at 550 K for alloys with 0.3% PbTe might be due to a combination of increased Seebeck coefficient and a substantially reduced thermal conductivity. That leads to the highest ZT value of 0.64.

Further increase of the ZT is possible due to annealing of the materials. So for comparison, samples with a concentration of PbTe of about 0.3 at% were analyzed, which were prepared by the melt spinning process.

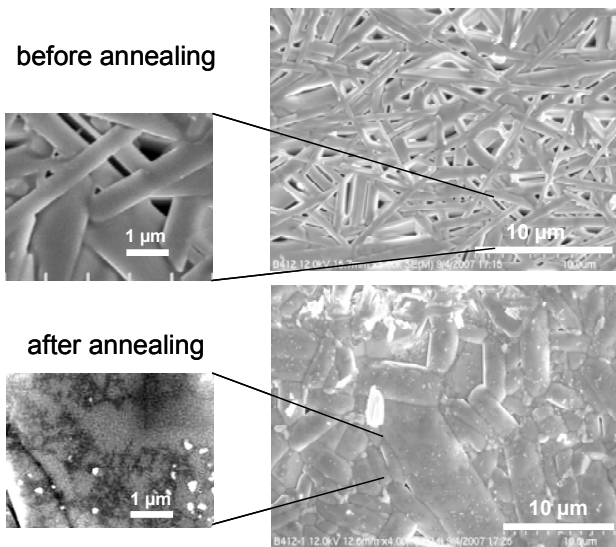


Fig. 7: Scanning electron micrographs indicating the improvement of the melt spin prepared p-type material $(Bi_{0.2}Sb_{0.8})_2Te_3$ with 0.3 at% of PbTe by annealing 1h at 680°C under nitrogen.

Figure 7 shows SEM pictures of the surface of such a sample before and after annealing. The as grown material exhibits a network like structure of needles with a diameter of about 1 μm . After annealing this structure has become more compact and the inset shows clearly more or less oriented structures of precipitations in the nm-range.

That change of the structure is also reflected in the thermoelectrical properties of the material, shown in figure 8. The electrical conductivity remains more or less the same after annealing ($1000 - 1300 (\Omega \cdot cm)^{-1}$) and is slightly higher compared to the in water quenched material

(about $1000 (\Omega \cdot cm)^{-1}$). More interesting is the substantial improvement of the Seebeck coefficient from about 120 $\mu V/K$ (the quenched and the meltspin material are the same) to about 160 $\mu V/K$ by annealing the melt spin material. After annealing a power factor of $\sim 34 \mu W/K^2 \cdot cm$ was obtained.

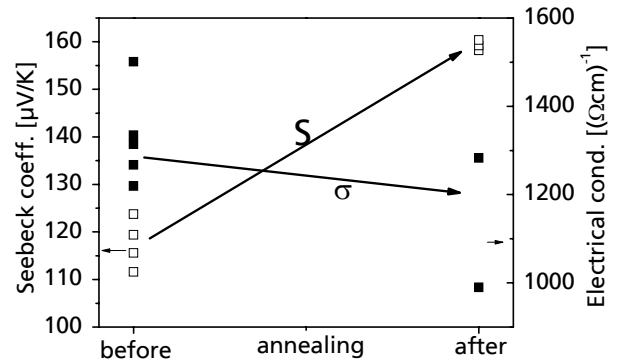


Fig. 8: Improvement of the electrical conductivity for p-type $(Bi_{0.2}Sb_{0.8})_2Te_3$ prepared by the melt spinning method due to annealing 1h at 680 K.

It could be shown, that the nanocomposite structure improves the thermopower and the thermal behaviour and ZT values above 1 were already obtained. The detailed results will be published elsewhere.

4. MODULE FABRICATION

The final step is the production of modules to be integrated into the wireless sensor systems. Therefore, the SPS-wafers of p- and n-type material were coated with Ni and Au, cut into peaces of $1.5 \times 1.5 \times 2 \text{ mm}^3$ to form the “legs”, which were soldered to Ni/Cu-plated standard alumina-substrates.

To optimize the thermogenerator modules and to study the influence of material properties on the performance according to the anisotropy of the SPS wafers, modules were built from legs, that were cut perpendicular and in plane of the wafer surface, see also figure 4. Only the n-type legs were fabricated randomly oriented, p-type legs were always perpendicular oriented to the wafer surface; the modules are shown in Figure 10. The

modules were improved according to their resistivity, which was reduced by about 30% showing a total resistance of 3.2 to 3.7 Ω . The Seebeck coefficient was improved about 10% to 185 $\mu\text{V}/\text{K}$, and the figure of merit of the module was improved by about 20% giving an overall module ZT of 0.5. No difference could be seen due to the different orientations. One explanation for this unexpected behavior are based on different contact properties, which may overrule the anisotropic material properties.



Fig. 10: Thermoelectric modules with preferential orientation (not oriented modules of the first generation (left) are compared to more recent modules, where the n-type legs are oriented in parallel (right) or perpendicular (middle) to the wafer surface).

Modules were integrated into a transfer system for wireless data, powered by human heat giving a temperature difference of 6°C. The temperature of the “hot side” is measured and is transmitted wireless together with the data of the power source to a laptop as can be seen in figure 11. The thermo generator produced a voltage of 206 mV with a current of 12.7 mA, giving a power of about 2.6 mW, more than sufficient to supply the sensor and wireless module, which needs together on average a power of about 1 mW, including the pulsed transceiver RF unit.

5. CONCLUSION

It could be demonstrated that melt spin fabrication can exhibit relatively high Seebeck coefficients of more than 200 $\mu\text{V}/\text{K}$ at RT after annealing. Although the process parameters of the melt spinning process do not remarkably influence the properties of the material, both p- and n- Bi_2Te_3 materials are improved after annealing substantially and exhibit higher Seebeck coefficients and better electrical conductivity.

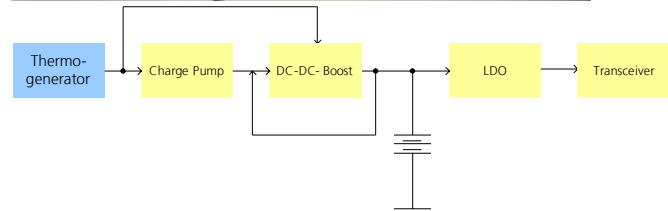
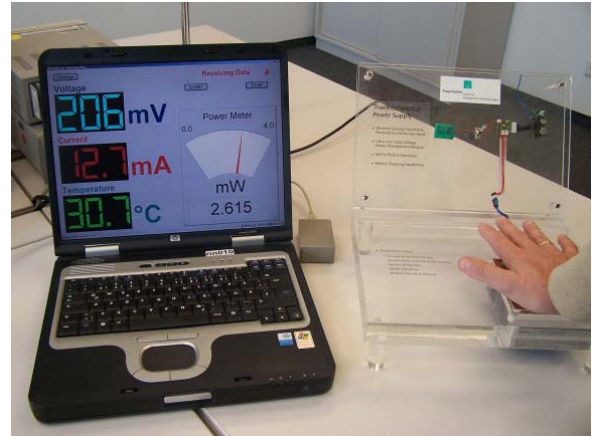


Fig. 11: Demonstration system for wireless sensing supplied with thermoelectrics. Underneath there is the block diagram for the energy management, sensing and wireless transmission.

The SPS-wafers show clear anisotropic behaviour and the figure of merit is improved according to a factor of ~ 2 up to $ZT=0.92$. At the same time the mechanical stability could be improved by the SPS process.

Alloying with PbTe was demonstrated to be another promising possibility to produce nanocomposites. For $(\text{Bi}_{0.2}\text{Sb}_{0.8})_2\text{Te}_3$ alloyed with up to 0.5% PbTe and quenched after melting in water the properties could already be improved for temperatures higher than RT. The thermal conductivity is significantly reduced and Pb-rich precipitations at grain boundaries of layered material were observed. An improvement for ZT of nearly 30% was achieved at RT and for temperatures of about 550 K an increase by a factor of 3 results in a ZT of about 0.64.

While the properties of water quenched materials and for melt spin material are more or less the same, a substantial improvement of the thermoelectric properties was observed due to annealing of melt spin material, giving a power factor as high as $\sim 34 \mu\text{W}/\text{K}^2\text{cm}$. The nanocomposite structure was shown by SEM for the best material with a composition of $[(\text{Bi}_{0.2}\text{Sb}_{0.8})_2\text{Te}_3]_{0.97}\text{PbTe}_{0.03}$ after annealing. This material offers the chance for ZT values $\gg 1$.

High quality spark plasma sintered wafers were obtained, showing a good homogeneity for thickness and thermoelectric properties.

Standard type modules were fabricated according to the orientation of the material, but the profits of the materials anisotropic properties were overruled probably by the contact behaviour of the material.

A first sensor system could fulfil the demands for wireless sensors supported by a temperature gradient of only 6 K, which gave a total power source of more than 2 mW. Signals can be sent wireless to a laptop without any additional energy source. Next step will be the miniaturizing of the system.

6. ACKNOWLEDGMENTS

This work was supported by the FhG Internal Programs under Grant No. WISA 815 020. The preparation of PbTe-alloyed samples is also acknowledged and was performed by the group of the LPM in Nancy, France, (Dr. Bertrand Lenoir) and by BASF in Ludwigshafen, Germany (Dr. Frank Haass).

7. REFERENCES

- [1] R. Venkatasubramanian et al., Thin-film thermoelectric devices with high room-temperature figures of merit, *Nature* Vol. 413 (2001), 597
- [2] T.C. Harman et al., Quantum Dot Superlattice Thermoelectric Materials and Devices, *Science* Vol. 297 (2002), 2229
- [3] K.F. Hsu et al., Cubic $\text{AgPb}_m\text{SbTe}_{2+m}$: Bulk Thermoelectric Materials with High Figure of Merit, *Science* Vol. 303 (2004), 818.
- [4] Jing Liu et al., Bi_2Te_3 and $\text{Bi}_2\text{Te}_3/\text{nano-SiC}$ Prepared by Mechanical Alloying and Spark Plasma Sintering, *Key Engineering Materials* Vols. 280-283 (2005), 397.
- [5] H. Y. Chen et al., Microstructures and thermoelectric properties of $\text{Fe}_{0.92}\text{Mn}_{0.08}\text{Si}_x$ alloys prepared by rapid solidification and hot pressing, *Journal of Applied Physics* Vol. 94 (2003), 6621.
- [6] E. Koukharenko et al., Electrical properties of $\text{Bi}_{2-x}\text{Sb}_x\text{Te}_3$ materials obtained by ultrarapid quenching, *Journal of Alloys and Compound* Vol. 327 (2001), pp. 1-4.
- [7] V.M. Glazov et al., Thermoelectric properties of semiconducting solid solution, $\text{Bi}_2\text{Te}_{2.4}\text{Se}_{0.6}$ $\text{Bi}_{0.52}\text{Sb}_{1.48}\text{Te}_3$ prepared by ultrafast cooling of melts, *Izv. Akad. Nauk, SSSR, Neorg. Mater.* Vol. 22, No. 1 (1986), pp 36-40.
- [8] E. Kukharenka et al., Electrical and microstructural properties of $\text{Bi}_{2-x}\text{Sb}_x\text{Te}$ and $\text{Bi}_{2-x}\text{Sb}_x\text{Te}_2$ foils obtained by ultrarapid quenching process, *Journal of Materials Science: Materials in Electronics* Vol. 14 (2003), pp. 383-388.
- [9] X. Tang et al., Preparation and thermoelectric transport properties of high-performance p-type Bi_2Te_3 with layered nanostructure, *Applied Physics Letters* Vol. 90 (2007), 012102.
- [10] T. Hirai et al., The pseudo-binary $\text{V}_2\text{VI}_3\text{-IV VI}$ compounds systems, $\text{Bi}_2\text{Te}_3\text{-PbTe}$, $\text{Bi}_2\text{Te}_3\text{-SnTe}$, $\text{Sb}_2\text{Te}_3\text{-PbTe}$, $\text{Sb}_2\text{Te}_3\text{-SnTe}$ and $\text{Bi}_2\text{Se}_3\text{-SnSe}$, *Journal of Less-Common Metals* Vol. 13 (1967), pp. 352-356,
- [11] E.I. Elagina et al., An investigation of the $\text{PbTe-Bi}_2\text{Te}_3$ and the $\text{SnTe-Sb}_2\text{Te}_3$ systems, *Russian Journal of Inorganic Chemistry* Vol. 4, No. 7 (1959), pp. 738-740.
- [12] D. Kusano et al., Effects of PbTe Doping on the Thermoelectric Properties of $(\text{Bi}_2\text{Te}_3)_{0.2}(\text{Sb}_2\text{Te}_3)_{0.8}$, *21st International Conference on Thermoelectrics* (2002), pp. 13-16.
- [13] P-W. Zhu et al., High thermoelectric properties of PbTe Doped with Bi_2Te_3 and Sb_2Te_3 , *Chinese Physics Letter* Vol. 28, No. 8 (2005), pp. 2103-2104
- [14] P. Zhu et al., Composition-Dependent Thermoelectric Properties of $(\text{PbTe})_{100-x}(\text{Bi}_2\text{Te}_3\text{-Sb}_2\text{Te}_3)_x$ ($0.1 \leq x \leq 5$), *Materials Transactions* Vol. 46, No. 4 (2005), pp. 761-764.
- [15] A. Golovanova et al., Interaction of Lead Telluride with Bismuth Telluride, *Neorganicheskie Materialy*, Vol. 19 No. 5, 1982
- [16] D.G. Ebling, A. Jacquot, H. Böttner, to be published
- [17] D.M. Rowe (edit.), *CRC Handbook of Thermoelectrics* CRC Press, Boca Raton, New York, London, Tokyo, 1995,